

# Molecular and Physiological Analysis of Arabidopsis Mutants Defective in Cytosolic or Chloroplastic Aspartate Aminotransferase<sup>1</sup>

Barbara H. Miesak and Gloria M. Coruzzi\*

Department of Biology, 100 Washington Square East, New York University, New York, New York 10003

Arabidopsis mutants deficient in cytosolic (AAT2) or chloroplastic (AAT3) aspartate (Asp) aminotransferase were characterized at the molecular and physiological levels. All of the ethyl methane sulfonate- or nitrosomethylurea-generated mutants are missense mutations, as determined by sequencing of the *ASP2* gene from the cytosolic *aat2* mutants (*aat2-1*, *aat2-2*, *aat2-4*, and *aat2-5*) and the *ASP5* gene from the chloroplastic *aat3* mutants (*aat3-1*, *aat3-2*, and *aat3-4*). A T-DNA insertion mutant in cytosolic AAT2 (*aat2-T*) was also identified. All the cytosolic *aat2* and chloroplastic *aat3* mutants have less than 6% AAT2 and less than 3% AAT3 activity, respectively, as determined by the native gel assay; however, none are nulls. The metabolic and physiological affect of these mutations in AAT isoenzymes was determined by measuring growth and amino acid levels in the *aat* mutants. Two *aat2* mutants (*aat2-2* and *aat2-T*) show reduced root length on Murashige and Skoog medium. For *aat2-2*, this growth defect is exaggerated by Asp supplementation, suggesting a defect in Asp metabolism. Amino acid analysis of the *aat* mutants showed alterations in levels of Asp and/or Asp-derived amino acids in several *aat2* alleles. Two *aat2* mutants show dramatic decreases in Asp and asparagine levels in leaves and/or siliques. As such, the cytosolic AAT2 isoenzyme appears to serve a nonredundant function in plant nitrogen metabolism of Asp and Asp-derived amino acids.

Nitrogen, often the rate-limiting element in plant growth, is first assimilated into the amino acids Glu and Gln by glutamine synthetase/glutamate synthase, and later into Asp and Asn by aspartate aminotransferase (AAT) and asparagine synthetase (AS; Lam et al., 1994, 1995; Stitt, 1999; Hirel and Lea, 2001). These four amino acids are used to transport nitrogen throughout the plant and represent 70% total free amino acids in Arabidopsis (Lam et al., 1995). Asp is amidated to form Asn when carbon skeletons are limiting, i.e. in the dark (Lam et al., 1994, 1998; Schultz et al., 1998). Asn is used as a nitrogen transport amino acid and to store nitrogen due to its high nitrogen:carbon ratio (2:4), compared with Gln (2:5; Urquhart and Joy, 1981; Lam et al., 1995). Thus, Asp formed by AAT plays a significant role in plant nitrogen assimilation and transport.

The AAT enzyme is a homodimer and binds the cofactor, pyridoxal phosphate, which then catalyzes the reversible reaction: oxaloacetate + Glu > < Asp +  $\alpha$ -ketoglutarate, ultimately regulating the synthesis or catabolism of Asp. Each AAT subunit contains one active site that functions independently of each other (Kirsten et al., 1983). AAT is encoded by a small gene family in Arabidopsis consisting of five genes, *ASP1* through 5 (for *ASP1-4*, see Schultz and Coruzzi, 1995;

for *ASP5*, see Wilkie et al., 1995). The predicted subcellular location for the AAT enzyme encoded by each *ASP* gene is predicted based on sequence analysis, in vitro chloroplast uptake (for *ASP5*), and assay of subcellular fractions on native gel followed by an AAT activity staining (Schultz and Coruzzi, 1995; Wilkie et al., 1995). The five *ASP* genes of Arabidopsis are predicted to encode isoenzymes for cytosolic AAT2 (*ASP2* and *ASP4*), chloroplastic AAT3 (*ASP5*), and mitochondrial AAT1 (*ASP1*). *ASP3* is believed to encode either a peroxisomal AAT or a minor chloroplastic AAT. Non-denaturing protein gels stained for AAT activity demonstrate there are three major detectable isoenzyme activities for AAT expressed in Arabidopsis, corresponding to mitochondrial (AAT1), cytosolic (AAT2), and chloroplastic (AAT3) isoenzymes (Schultz and Coruzzi, 1995).

The various AAT isoenzymes may play specific roles in: (a) converting newly formed organic nitrogen to the nitrogen carriers, Glu and Asp; (b) the formation of Asp used to generate several essential amino acids such as Asn, Met, Thr, and Ile; (c) the regeneration of carbon skeletons ( $\alpha$ -ketoglutarate) for further primary nitrogen assimilation; (d) the assimilation of organic nitrogen compounds formed from photorespiration; and (e) the shuttling of reducing equivalents between cells (for review, see Given, 1980; Cooper and Meister, 1985).

Using a screen for loss-of-enzyme activity, Arabidopsis mutants defective in either cytosolic AAT2 (*aat2-1*, *aat2-2*, *aat2-4*, and *aat2-5*) or chloroplastic AAT3 (*aat3-1*, *aat3-2*, and *aat3-4*) were isolated, and the mapping of *ASP* genes and *aat* mutants was

<sup>1</sup> This work was supported by the National Science Foundation (grant no. MCB 98-17900 to G.M.C.).

\* Corresponding author; e-mail gloria.coruzzi@nyu.edu; fax 212-995-4204.

Article, publication date, and citation information can be found at [www.plantphysiol.org/cgi/doi/10.1104/pp.005090](http://www.plantphysiol.org/cgi/doi/10.1104/pp.005090).

carried out (Schultz et al., 1998). Mapping analysis indicated that the *aat* mutants in cytosolic AAT2 are linked to *ASP2*, whereas those in chloroplastic AAT3 are linked to the *ASP5* gene. In this report, we characterize the molecular and phenotypic defects in five allelic *aat2* mutants in cytosolic AAT2 and three allelic *aat3* mutants in chloroplastic AAT3. Although all of the mutants are defective in AAT isoenzyme activity, the mutants have varied phenotypic effects with regard to growth, Asp metabolism, and amino acid profiles, as described herein. Cytosolic AAT2 appears to play a nonredundant role because two *aat2* mutants show dramatic Asp-related defects in amino acid profiles and growth.

## RESULTS

New alleles of mutants defective in cytosolic AAT2 or chloroplastic AAT3 were identified using a gel-based activity stain. In wild-type Arabidopsis, the predominant isoenzymes of AAT found in a crude protein extract and assayed by native gel electrophoresis are cytosolic AAT2 and chloroplastic AAT3 (Fig. 1A, lane 1). Previously, it was shown that mutants lacking these isoenzymes could be isolated using the gel-based assay to detect AAT activity (Schultz et al., 1998). To identify potential null alleles in the *ASP* genes encoding AAT isoenzymes, this method was used to screen for additional individuals

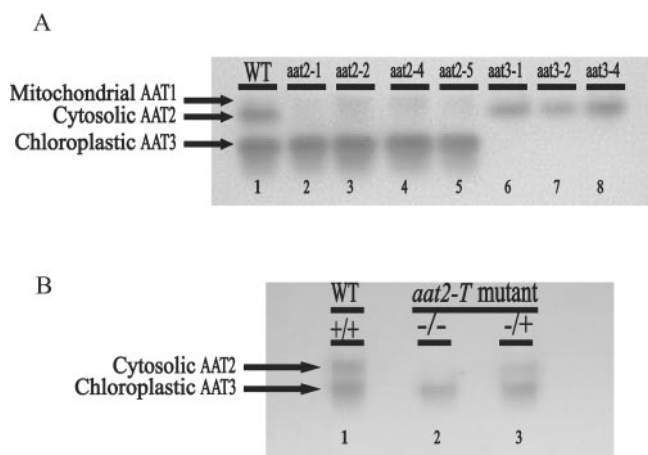


**Figure 1.** AAT activity gel of wild-type and mutant plants. Arabidopsis ecotype Columbia (Col; wild type) plant protein extracts run on native gels stained for AAT activity show two major and one minor AAT isoenzyme activity bands: mitochondrial AAT1, cytosolic AAT2, and chloroplastic AAT3. A, Lane 1 represents AAT activity in wild-type Arabidopsis, lanes 2 through 5 represent Arabidopsis mutants in cytosolic AAT2, and lanes 6 through 8 represent Arabidopsis mutants in chloroplastic AAT3. The additional new mutants, cytosolic *aat2-5* and chloroplastic *aat3-4*, were isolated from individual pools of nitrosomethylurea (NMU)-mutagenized seed. B, AAT activity gel of an *ASP2* T-DNA-inserted mutant (*aat2-T*) shows loss of cytosolic isoenzyme activity (lane 2) compared with wild type (lane 1). The mutant hemizygous for the *ASP2* T-DNA insertion (lane 3) has one-half of the WT AAT2 activity and reflects the dose effect of having one wild-type *ASP2* gene.

defective in either cytosolic AAT2 or chloroplastic AAT3 in ethyl methane sulfonate-/NMU-mutagenized seeds. In this assay, cytosolic *aat2* mutants are detected by a reduction in the cytosolic AAT2 activity band (Fig. 1A, lanes 2–5), whereas chloroplastic *aat3* mutants have reduced levels of the AAT3 activity band (Fig. 1A, lanes 6–8). Previous dilution studies showed that the native gel assay can detect as low as 6% of wild-type activity for cytosolic AAT2 and 3% of wild-type activity for chloroplastic AAT3 (Schultz et al., 1998). None of the *aat* mutant lines contain any detectable cytosolic AAT2 or chloroplastic AAT3 activity, respectively (Fig. 1A). The faint band above AAT2 in Figure 1A, lanes 2 through 5, represents mitochondrial AAT1, which is a minor AAT component only visible when gels are overloaded (Schultz and Coruzzi, 1995).

Using this gel-based method, two new *aat* mutants were isolated from separate pools of NMU-mutagenized seed. One individual isolated was defective in cytosolic AAT2 (*aat2-5*, Fig. 1A, lane 5), whereas the other individual was defective in chloroplastic AAT3 (*aat3-4*, Fig. 1A, lane 8).

### Identification of T-DNA-Inserted *aat2* Mutant Using a PCR-Based Screen

In an attempt to identify null mutations defective in AAT2 or AAT3, 60,480 T-DNA inserted lines were screened by PCR using gene-specific primers to the corresponding *ASP* genes (*ASP2* and *ASP5*) and left border of the T-DNA insert (Krysan et al., 1999). A mutant containing a T-DNA insertion in the *ASP2* gene (*aat2-T*) was identified using primers specific to cytosolic *ASP2*. The T-DNA was determined to be located in intron 8 of the *ASP2* gene. The hemizygote (*AAT2/aat2-T*) segregates in a 3:1 ratio of resistance to sensitivity on 100 mg mL<sup>-1</sup> kanamycin, indicating there is one locus of T-DNA insertion in the genome. To determine whether the *aat2-T* mutant was defective in AAT activity, crude protein extracts from *aat2-T* homozygotes and hemizygotes were run on native gels and stained for AAT activity (Fig. 1B). The AAT activity was compared with the AAT activity in wild-type plants on the native gel as a positive control (Fig. 1B, lane 1). Homozygous *aat2-T* mutants showed no detectable cytosolic AAT2 activity (Fig. 1B, lane 2), whereas the hemizygous *aat2-T* mutants (*AAT2/aat2-T*) showed approximately one-half of the wild-type AAT2 activity (Fig. 1B, lane 3). Thus, the AAT gel-based assay shows a dose effect of having one functional *ASP2* gene, as shown previously (Schultz et al., 1998).

### Determination of *ASP* mRNA Levels in *aat* Mutants

The *aat2-T* mutant is deficient in AAT2 based on native gels stained for AAT activity (Fig. 1B, lane 2). AAT activity gels can detect down to 6% AAT2 ac-

tivity with potentially less than 6% AAT2 activity remaining. The possibility that there is some AAT2 activity present in *aat2-T* below the sensitivity of detection by native gels is supported by the finding that there is residual *ASP2* mRNA in the mutant. However, in *aat2-5*, the T-DNA insertion is located in an intron, leading to the possibility that a functional mRNA could be formed if the T-DNA is spliced out. Semiquantitative reverse transcriptase (RT)-PCR was used to detect *ASP2* mRNA because it is a more sensitive method for determining whether there is mRNA made, as compared with northern analysis. To determine if splicing of the T-DNA out of the *ASP2* mRNA occurs, RT-PCR was performed on mRNA from *aat2-T* (Fig. 2, lane 5). Primers designed to span the region containing the T-DNA insertion in the *aat2-T* mutant were used for RT-PCR. This analysis showed that some *ASP2* transcript is properly processed in *aat2-T* (*ASP2* intron-containing T-DNA is spliced out of the *aat2-T* mutant), as indicated by the presence of a PCR product of wild-type size (Fig. 2, lane 5). However, the relative level of the *ASP2* transcript is lower in *aat2-T* than in wild-type plants (Fig. 2, lane 4). This could reflect a less efficient processing or destabilization of *ASP2* mRNA in *aat2-T* compared with wild type. This difference in transcript level between *aat2-T* and wild-type plants can also be detected using semiquantitative RT-PCR (Fig. 2, cycle 25, lanes 2 and 1, respectively) and comparing to amplification of wild-type amplification of an internal control gene (*ASP5*). RT-PCR, a more sensitive mRNA detection than northern analysis, was performed on *aat2-5*, an allele shown to have reduced mRNA levels by northern analysis (data not shown). The RT-PCR amplification, corresponding to the *ASP2* transcript levels, is moderately less intense in *aat2-5* (Fig. 2, lanes 3 and 6) than in

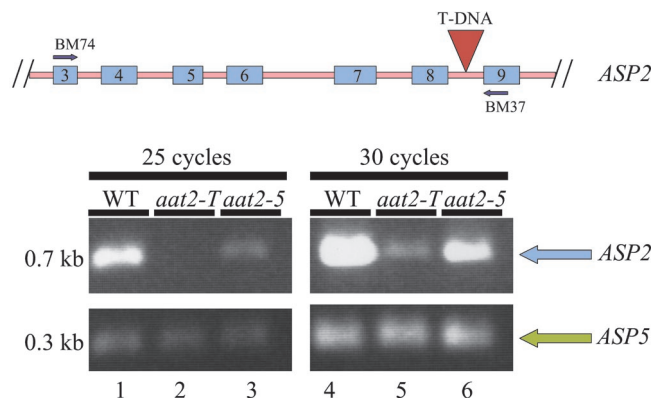


**Figure 2.** Semiquantitative RT-PCR of *ASP2* mRNA in *aat2* mutants. A schematic drawing of the *ASP2* gene including exons 3 through 9 (blue) and introns (pink) indicates where the T-DNA insertion is located (red) and the oligonucleotide primers on the *ASP2* gene used in the RT-PCR (BM74 and BM37). PCR was performed for 25 cycles (lanes 1–3) or for 30 cycles (lanes 4–6) on wild type (lanes 1 and 4), *aat2-T* (lanes 2 and 5), and *aat2-5* (lanes 3 and 6). Co-Amplification of *ASP5* was used as a positive control in the same PCR reaction tube.

**Table 1.** Missense mutations in cytosolic *ASP2* or chloroplastic *ASP5* genes of *aat* mutants

Isoenzyme	Mutant Allele	Affected Gene	Missense Mutation
Cytosolic AAT2	<i>aat2-1</i>	<i>ASP2</i>	G254R
	<i>aat2-2</i>	<i>ASP2</i>	P71L
	<i>aat2-4</i>	<i>ASP2</i>	P46L
	<i>aat2-5</i>	<i>ASP2</i>	S306N
Chloroplastic AAT3	<i>aat3-1</i>	<i>ASP5</i>	P118S
	<i>aat3-2</i>	<i>ASP5</i>	G342E
	<i>aat3-4</i>	<i>ASP5</i>	G156S

wild type (Fig. 2, lanes 1 and 4, respectively). Amplification of *ASP5* was utilized as an internal control (Fig. 2). All other *aat2* and *aat3* alleles had normal levels of *ASP* mRNA as determined by northern blot (data not shown).

### Identification of Molecular Lesions in *aat* Mutants

Previously, we showed that the cytosolic *aat2* mutants and the *ASP2* gene are genetically linked (Schultz et al., 1998). Here, we define the molecular lesions in the *ASP2* gene of the cytosolic *aat2* mutants. Similarly, we previously showed that the chloroplastic *aat3* mutants and the *ASP5* gene for chloroplastic AAT3 are genetically linked (Schultz et al., 1998). Here, we identify the molecular lesions in the *ASP5* gene of the mutants defective in chloroplastic AAT3.

Sequencing of *ASP2* and *ASP5* structural genes from the cytosolic *aat2* or chloroplastic *aat3* mutants (Fig. 1A), respectively, showed that missense mutations occur in each of these mutants. The location and nature of the missense mutations are summarized in Table I and shown schematically in Figure 3. Three of the *aat* mutants have an amino acid change from Gly to Arg (*aat2-1* G254R), Glu (*aat3-2* G342E), or Ser

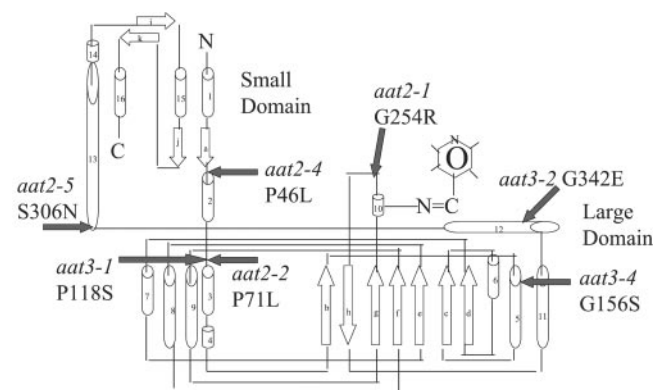


**Figure 3.** Location of missense mutations in AAT enzyme of *aat* mutants. A schematic drawing of an AAT subunit with  $\alpha$ -helices represented as barrels,  $\beta$ -sheets represented as white block arrows, with small and large domains and the pyridoxal phosphate-binding site indicated (adapted from Wilkie et al., 1996). Positions of altered amino acids located in cytosolic *aat2* and chloroplastic *aat3* missense mutants are indicated by filled black arrows.



(*aat3-4* G156S). Three of the *aat* mutants have an amino acid change from Pro to Leu (*aat2-2* P71L and *aat2-4* P46L), or to Ser (*aat3-1* P118S). *aat2-5* (S306N) has an amino acid change from Ser to Asn. In Figure 3, these missense mutations are mapped onto a schematic diagram of AAT enzyme derived from Wilkie et al. (1996).

#### Asp-Supplemented Medium Shows an Asp-Induced Growth Defect in the *aat2-2* Mutant

Our previous studies showed that *aat2-2*, which is defective in Asp accumulation, exhibits a growth defect when grown on Murashige and Skoog medium (Schultz et al., 1998). Here, we show a similar growth defect for *aat2-2* and a second allele *aat2-T* (Fig. 4A). To determine whether the growth defect observed in *aat2-2* and *aat2-T* mutants is related to an Asp deficiency, we tested whether this growth defect could be rescued by exogenously supplied Asp. To test this, *aat2* mutant plants (*aat2-2* and *aat2-T*) and wild type were grown on Murashige and Skoog medium supplemented with Asp (0 mM and 20 mM; Fig. 4, A and B). Growth of *aat2* mutant plants was compared with wild type by measuring root length. Root length of *aat2-2* and *aat2-T* was shorter than wild type when grown on Murashige and Skoog medium, in the absence of any Asp supplementation (Fig. 4A). Surprisingly, when 20 mM Asp was added to the growth medium, growth impairment in *aat2-2* was exaggerated, whereas wild-type growth was relatively unimpaired (Fig. 4, A and B), indicating that the *aat2-2* mutant has an Asp-dependent growth defect. The newly isolated T-DNA mutant in *ASP2*, *aat2-T*, also displayed a significant growth impairment indicated by the *P* value ( $P < 0.05$ ) on Murashige and Skoog growth medium, similar to the growth defect shown in *aat2-2* as compared with wild type (Fig. 4A). However, this growth impairment found in *aat2-T* was not exaggerated by the addition of exogenous Asp. Surprisingly, wild-type plants were mildly impaired on 20 mM Asp, whereas *aat2-T* plants were unimpaired (Fig. 4A), suggesting that either *aat2-T* may be mildly resistant to Asp treatment or that a larger sampling of wild-type plants would lead to less variability. No growth defects were observed in the other *aat2* and *aat3* mutants (data not shown).

#### Determination of Levels of Free Asp and Asp-Derived Amino Acids in *aat2* and *aat3* Mutants

Amino acid analysis was performed to determine whether a mutation in cytosolic AAT2 or chloroplastic AAT3 affected levels of free Asp or Asp-derived amino acids. Seedlings were grown on Murashige and Skoog media for 7 d in continuous light or in continuous dark (see "Materials and Methods"). Lev-

els of the transported amino acids Glu, Gln, Asp, and Asn are shown in Figure 5, A and B.

Asp levels in wild-type plants are higher in the light than in the dark (Fig. 5, A and B, lane 1). In contrast, Asn levels are higher in the dark than in the light of wild-type plants (Fig. 5, A and B, lane 11). Only the *aat2-2* mutation shows a reduction in the levels of free Asp in light-grown plants (Fig. 5A, lane 2). Levels of Asp in etiolated plants are normal in *aat2-2* (Fig. 5B, lane 2). Levels of Asp are wild type in all other *aat2* and *aat3* mutant alleles in plants grown in the light or dark. The level of the Asp-derived amino acid, Asn, is decreased in the dark-grown *aat2-2* plants (Fig. 5B, lane 12). This supports our previous model that pools of Asp synthesized in the light by AAT2 are utilized for the synthesis of Asn in the dark (Schultz et al., 1998). Although *aat2-T* does not show a decrease in Asp levels in light-grown plants (Fig. 5A, lane 4), it does show a dramatic decrease in Asn levels in dark-grown plants (Fig. 5B, lane 14). The levels of Glu in the light are higher for *aat2-T* (Fig. 5A, lane 9) compared with wild type (Fig. 5A, lane 6). The other *aat2* and *aat3* mutants showed little change in Glu from wild type in light- or dark-grown plants (Fig. 5A, lanes 7, 8, and 10). The level of Gln is higher in all *aat2* and *aat3* mutants in both light-grown (Fig. 5A, lanes 17–20) and etiolated plants (Fig. 5B, lanes 17–20) compared with wild-type light-grown (Fig. 5A, lane 16) or etiolated (Fig. 5B, lane 16) plants.

Silques contain the pools of amino acids used in the synthesis of seed proteins and Asp is an import amino acid used to transport nitrogen from sources to sinks. To determine if levels of Asp and Asp-derived amino acids were affected in siliques, we performed HPLC analysis of siliques for wild-type and *aat* mutants. Siliques from two cytosolic *aat2* mutants (*aat2-2* and *aat2-5*) had significant reductions in Asp (Fig. 6, lanes 2 and 3), Glu (Fig. 6, lanes 7 and 8), and Asn (Fig. 6, lanes 12 and 13), compared with wild type (Fig. 6, lanes 1, 6, and 11). In contrast, Gln levels were higher in siliques of all three *aat2* mutants (Fig. 6, lanes 17–19) compared with controls (Fig. 6, lane 16). Surprisingly, Asp levels in siliques from *aat2-T* (Fig. 6, lane 4) were not different from wild type (Fig. 6, lane 1), whereas levels of Asn were dramatically decreased (Fig. 6, lane 14). Chloroplastic *aat3* mutants (*aat3-1*, *aat3-2*, and *aat3-4*) showed no changes in levels of the amino acids Asp and Asn compared with wild type in whole-plant extracts of leaves and siliques (Figs. 5 and 6) or in isolated chloroplasts (data not shown).

#### DISCUSSION

Eight mutants in cytosolic AAT2 or chloroplastic AAT3, deficient in the major AAT isoenzymes in Arabidopsis, were used to study the role of these enzymes in plant nitrogen metabolism. Seven of the

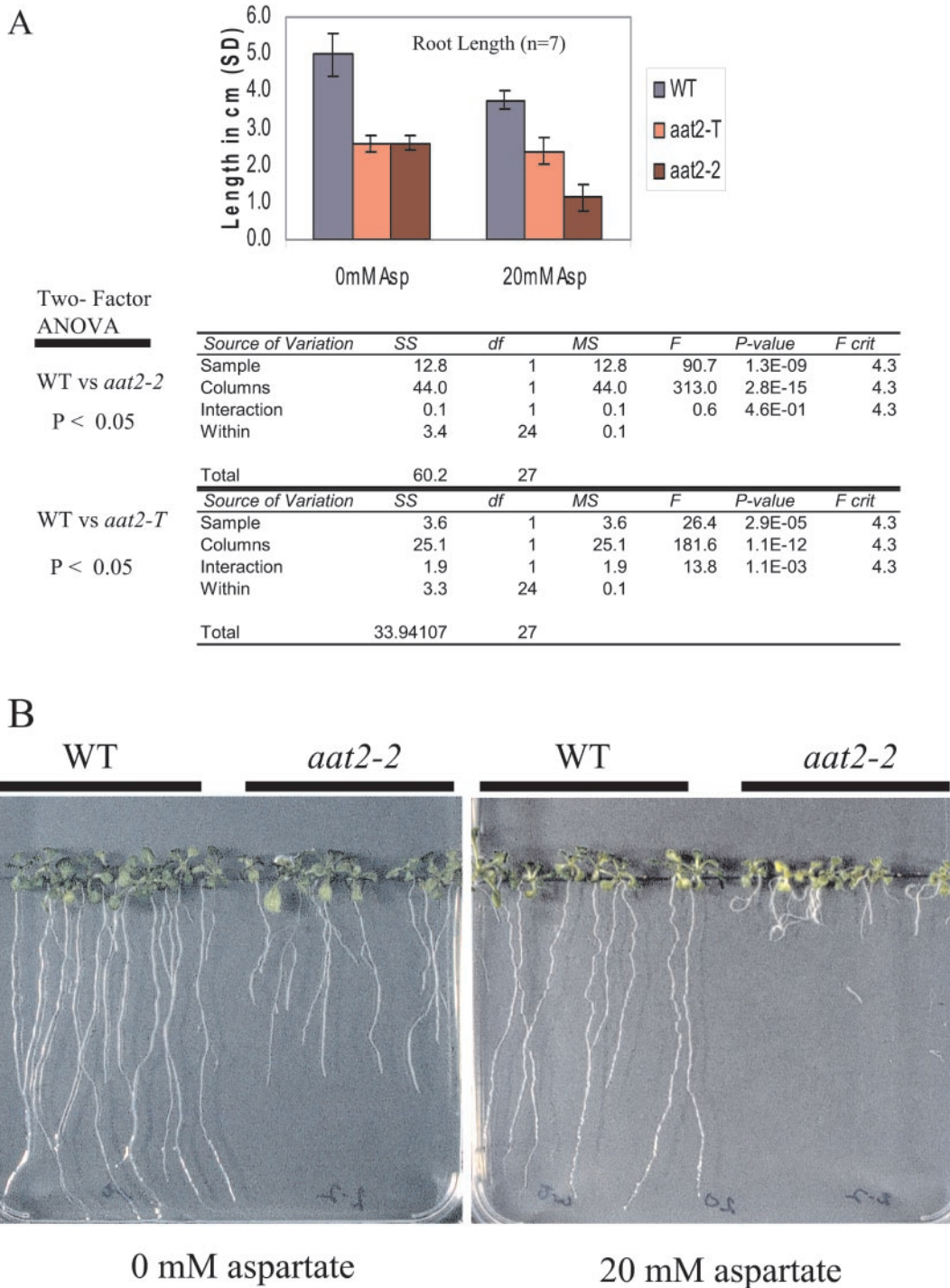


**Figure 4.** Asp-related growth defect in cytosolic *aat2* mutants. A, *aat2-T* mutant plants were grown on Murashige and Skoog medium supplemented with 0 and 20 mM Asp and the root lengths were measured and compared with *aat2-2* mutant and wild-type plants. A two-way ANOVA is shown ( $P < 0.05$ ;  $n = 7$ ). B, *aat2-2* mutants and wild-type plants were grown on medium without supplemented Asp and medium supplemented with 20 mM Asp.

*aat* mutants identified from separate pools of ethyl methane sulfonate-/NMU-mutagenized seed represented two complementation groups: cytosolic AAT2 (*aat2-1*, *aat2-2*, *aat2-4*, and *aat2-5*) and chloroplastic AAT3 (*aat3-1*, *aat3-2*, and *aat3-4*). Four *aat* mutants

are missense mutations in the *ASP2* gene for cytosolic AAT2 and three *aat* mutants are missense mutations in the *ASP5* gene for chloroplastic AAT3 (Table I). The eighth mutant, *aat2-T*, isolated from T-DNA inserted lines, has a T-DNA insertion in intron 8 of

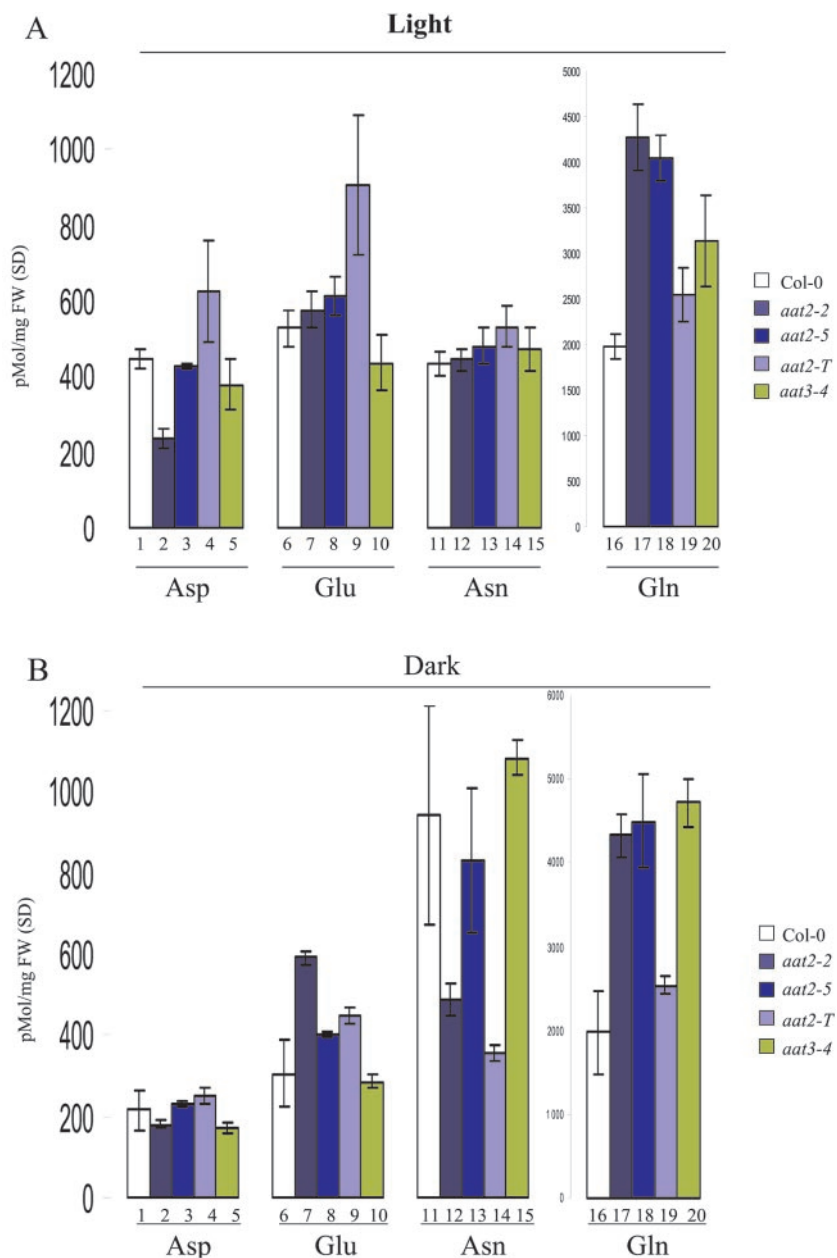


**Figure 5.** HPLC analysis of Asp, Asn, Glu, and Gln levels in *aat* mutants. The levels of free amino acids were measured in cytosolic *aat2* (blue bars) and chloroplastic *aat3* (green bars) mutants and wild-type plants (white bars) using HPLC analysis. Plants were grown on Murashige and Skoog plates in continuous light or continuous dark for 7 d ( $n = 3$ ). Each data point represents an extract from whole seedlings collected from different plates and is a biological replicate ( $n = 3$ ). All error bars in the HPLC analyses represent sds of biological replicates.

*ASP2*. This was determined to be a leaky mutant based on RT-PCR analysis. Although the missense mutations in the *ASP* genes of the missense mutants are not in residues previously described to be important for function by mutational analyses on AAT in other organisms, they do represent nonconservative substitutions of amino acids positioned near these conserved regions of functional significance (Mehta et al., 1989; Smith et al., 1989; Kamitori et al., 1990; Goldberg et al., 1991; Udvardi and Kahn, 1991; Inoue et al., 1991; Pan et al., 1993; Ziak et al., 1993; Okamoto et al., 1994; Kohler et al., 1994; Wilkie et al., 1996). To locate the domains of AAT affected by the *aat* missense mutations, the location of each missense mutation was mapped onto a schematic representation of

a subunit of the AAT homodimer from Arabidopsis (Fig. 3). The numbering of the amino acid residues in *aat3* begins with the chloroplastic transit peptide consisting of 47 residues.

The AAT subunit, in Arabidopsis, contains a small domain made from two regions of the polypeptide (N terminus to Pro-94 and Arg-369 to the C terminus), a large domain (the remaining polypeptide), an  $\alpha$ -helix connecting the two domains (Val-351 to Ser-383), and a pyridoxal phosphate cofactor-binding site at Lys-298 (Wilkie et al., 1996). Both the small and the large domains are involved in the function of the AAT enzyme, where binding of the cofactor, pyridoxal phosphate, is involved in both the forward and the reverse reactions. The active site of each subunit



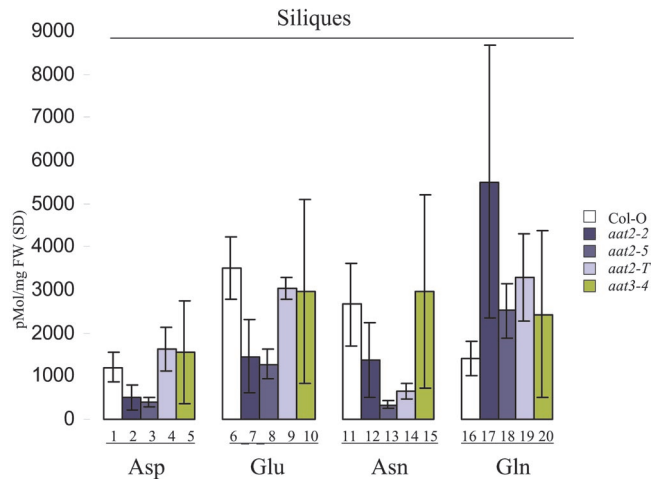


**Figure 6.** HPLC analysis of Asp, Asn, Glu, and Gln in the siliques of *aat* mutants. The levels of free amino acids in cytosolic *aat2* (blue bars) and chloroplastic *aat3* (green bars) and wild-type plants (white bars) were analyzed in siliques using HPLC ( $n = 3$ ). Each individual represents a biological replicate. All errors in the HPLC analyses represent biological replicates.

consists of the small and large domains and the large domain of the second subunit contributing to one wall of the active site (McPhalen et al., 1992). Residues in both the small and large domain contribute to substrate binding and stability of the cofactor (McPhalen et al., 1992). Each AAT subunit contains one active site and their activities of substrate binding and catalysis occur independently of each other (Kirsten et al., 1983). A conformational change occurs in the small domain on substrate binding to the cofactor in the large domain, binding the substrate snugly in the active site (McPhalen et al., 1992). The subunit interface, consisting of the subunit interface residues that stabilize the enzyme in its active dimeric form, is unusually large, indicating a stable dimer (McPhalen et al., 1992). The three-dimensional structure of an enzyme defines the substrate specificity and its function (Hrmova and Fincher, 2001).

In the *Arabidopsis aat2* and *aat3* mutants described herein, small domain mutations occur in *aat2-4* (P46L), and large domain mutations are located in *aat2-1* (G254R), *aat2-2* (P71L), *aat3-1* (P118S), *aat3-2* (G342E), and *aat3-4* (G156S). The mutation in *aat2-5* (S306N) is located in the region joining the small and large domains. *aat2-1* (G254R) is located three residues from the Lys residue that binds the cofactor pyridoxal phosphate (Fig. 3). Mutations in these residues are either required for the activity of the AAT enzyme or affect protein stability because each of these mutations result in reduction in levels of cytosolic AAT2 activity in the *aat2* mutants and the reduction in levels of chloroplastic AAT3 activity in the *aat3* mutants (Fig. 1A). The AAT activity gels indicate that all the mutants contain less than 6% cytosolic AAT2 activity in the *aat2* mutants and less than 3% chloroplastic AAT3 activity in the *aat3* mutants. The

variable growth results and amino acid levels in these *aat* mutants may reflect differences in AAT activity levels below these lower limits of detection, or differences in penetrance of the distinct missense mutations occurring in different regions of the *ASP2* or *ASP5* genes. The *aat2-2* mutant affected in the major gene encoding cytosolic AAT2 seems to be the most severely affected *aat* mutant allele. *aat2-2* exhibits an impaired growth phenotype as seen by short roots compared with wild-type plants (Fig. 4A). This growth defect is exaggerated when *aat2-2* is grown on medium supplemented with Asp, suggesting that the enhanced growth defect is related to Asp metabolism (Fig. 4, A and B).

The *aat2-2* mutant allele also has Asp-related defects in its amino acid profile. Previously, we showed the *aat2-2* mutant has reduced levels of Asp in 4-week-old 24-h light-adapted plants, indicating a role for cytosolic AAT2, in the synthesis of the bulk of Asp in the light (Schultz et al., 1998). Here, we show *aat2-2* has reduced levels of Asp in 7-d light-grown plants, as well as reduced levels of Asn in 7-d etiolated mutants compared with wild-type controls (Fig. 5). This supports the previous model in which cytosolic AAT2 is predicted to be responsible for synthesizing the bulk of Asp in the light, which supplies the precursor for Asn synthesis in the dark (Schultz et al., 1998). In addition, we have shown that *aat2-2* has dramatic decreases in levels of Asp and Asn in siliques (Fig. 6), indicating a new role for cytosolic AAT2 for the synthesis of Asp/Asn for seed storage. Levels of the AAT2 holoenzyme are high in siliques of wild-type plants, and reduced in siliques of *aat2* mutants (*aat2-2*, *aat2-5*, and *aat2-T*, data not shown). Thus, it is likely that cytosolic AAT2 may serve to synthesize Asp in situ in siliques. However, this does not preclude the possibility that AAT2 activity in leaves also provides Asp that is transported to siliques (Fig. 7).

A second mutant in cytosolic AAT2, *aat2-5*, has reduced levels of *ASP2* transcript at the level of northern analysis and RT-PCR (Fig. 2). It is unclear how a missense mutation might result in reduced mRNA levels. Other studies have shown decreased mRNA levels in Trp synthase beta subunit as a result of a missense mutation (*trp2-5*; Barczak et al., 1995). Although levels of Asp in *aat2-5* are not decreased in light-grown plants, levels of free Asp in siliques are decreased compared with wild type (Fig. 7), supporting a role for cytosolic AAT2 in the synthesis of Asp used for seed storage in developing siliques. This suggests that the Asp defect in siliques is due to a defect in Asp synthesis in situ, and not to Asp transported from leaves because levels of Asp are normal in leaves of the *aat2-5* plants (Fig. 5A, lane 3).

A T-DNA-inserted allele of *aat2* (*aat2-T*) was isolated with the intention of obtaining a null allele of *aat2*. The T-DNA in *aat2-T* is located in intron 8 of *ASP2*. However, some *aat2-T* transcript is properly

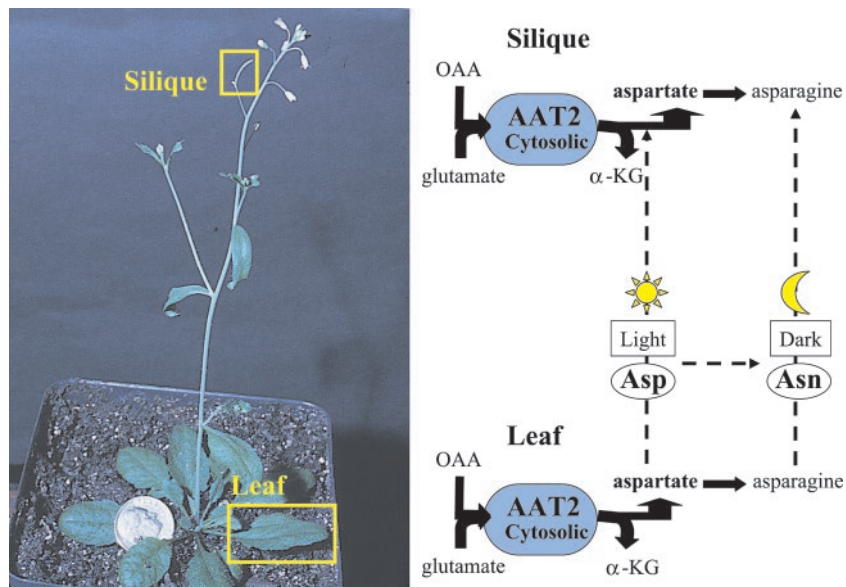


**Figure 7.** Cytosolic AAT2 activity in leaves and siliques. Cytosolic AAT2 activity occurs in both leaves and siliques *in situ*. Levels of Asp and Asp-related amino acids in siliques represent those made by AAT2 in siliques and possibly transported amino acids from leaves. Cytosolic AAT2, in the forward direction, utilizes Glu and oxaloacetate (OAA), leading to the synthesis of Asp, the precursor for Asn synthesis by AS, and alpha-ketoglutarate ( $\alpha$ -KG).

processed as judged by RT-PCR (Fig. 2). Semiquantitative RT-PCR performed at two cycling times shows reduced transcript for both *aat2-T* and *aat2-5* mutants compared with wild type, indicating this difference is not due to saturation of the PCR components. *aat2-T* exhibits an impaired growth phenotype as measured by short root length compared with wild-type plants on Murashige and Skoog plates. However, unlike the *aat2-2* mutant, the growth defect in *aat2-T* is not enhanced by Asp supplementation (Fig. 4A). Although levels of Asp are not defective in seedlings of *aat2-T*, there is a reduction in Asn in etiolated plants (Fig. 5). Unlike *aat2-2* and *aat2-5*, levels of Asp are not decreased in siliques of *aat2-T*. However, levels of Asn are decreased in siliques of *aat2-T*, as they are in *aat2-2* and *aat2-5*.

In summary, three independent mutants in cytosolic AAT2 (*aat2-2*, *aat2-5*, and *aat2-T*) are each defective in AAT2 activity in leaves and siliques. Siliques from two cytosolic *aat2* mutants (*aat2-2* and *aat2-5*) also show a reduction in free Asp, Glu, and increased levels of Gln compared with wild-type plants. The Gln “buildup” in the *aat2-2* and *aat2-5* mutants correlates with Asn decreases, suggesting that the mutants are impaired in converting Gln to Asp required for Asn synthesis. Levels of Asp-derived Asn are also decreased in siliques of all three *aat2* alleles, suggesting a role for Asp derived from cytosolic AAT2 in Asn synthesis in siliques. It is possible that the defect in levels of Asp-derived Asn is more observable because Asn is more metabolically inert than Asp. In addition, Asp levels detected in *aat2-T*, a mutant with decreased transcript compared with controls, may be synthesized by other aminotransferases. Our results suggest, however, that Asn synthesis is dependent on Asp synthesized by cytosolic AAT2 and that other pools of Asp cannot replace the defect caused by AAT2. This observation suggests that there is either

compartmentation of amino acid pools in plants, or that the AAT2 enzyme and the AS enzyme are part of a super complex to allow metabolic flux between this enzyme pair (for review, see Hrazdina and Jensen, 1992; Huang et al., 2001). Also, functional compartmentation where the enzymes are not physically associated has been implicated in the exchange of oxaloacetate between AAT and malate dehydrogenase (Salerno et al., 1985).

Although the mutants in cytosolic AAT2 showed Asp-related defects in HPLC and growth analyses, *aat3-4*, a mutant in chloroplastic AAT3, did not show defects in Asp synthesis in seedlings or siliques. Isolated chloroplasts and total plant extract from chloroplasts of a series of AAT3 mutant alleles (*aat3-1*, *aat3-2*, and *aat3-4*) are also unaltered in Asp and Asn levels compared with wild-type plants (data not shown). However, these *aat3* mutants are all missense mutants and not null mutants; therefore, at present we cannot conclude about the role of chloroplastic AAT3 in plant nitrogen metabolism.

In summary, cytosolic *aat2* and chloroplastic *aat3* mutants have various missense mutations in the enzyme, resulting in a spectrum of altered enzyme function that may be due to enzyme inactivation or enzyme instability. Asp-related phenotypes associated with mutants in cytosolic AAT2 (*aat2-2*, *aat2-5*, and *aat2-T*) indicate that this AAT isoenzyme plays a nonredundant role in Asp synthesis and metabolism in the cytosol of leaves and siliques, compared with other isoenzymes. Our studies suggest that cytosolic AAT2 is responsible for the bulk of Asp synthesis in the light and these Asp pools are utilized for the synthesis of Asn in the dark, and for Asp and the Asn levels in the siliques. These results demonstrate a nonredundant role for cytosolic AAT2 in the assimilation of nitrogen into Asp in the cytosol of leaves and siliques.



## MATERIALS AND METHODS

### Plant Material

Arabidopsis ecotype Col were used for all wild-type and mutant background tissue experiments except for the T-DNA-inserted ASP2 mutant, which was isolated from a Wassilewskija background. Both of the new *aat2* and *aat3* mutants were backcrossed to Col at least once to reduce background mutations.

All seeds were first sterilized in commercial bleach and 1% (v/v) Tween 20 for 2 min, washed three times, and imbibed in the dark at 4°C, before plating on Murashige and Skoog (Murashige and Skoog, 1962) plant medium supplemented with 1% (w/v) Suc and 0.9% (w/v) agar and grown in environmental growth chambers (EGC, Chagrin, OH) set on a 16-h-light (65  $\mu\text{E m}^{-2} \text{s}^{-1}$ )/8-h-dark cycle unless otherwise stated. Plant material used for the AAT enzyme activity gels (Fig. 1, A and B) and northern blots was first grown on Murashige and Skoog plates supplemented with 3% (w/v) Suc and 0.9% (w/v) agar. After 1 week, the plants for the AAT activity gel assay were transferred to soil for an additional 2 weeks before assaying for plant protein extract. For Asp supplementation plates, medium was supplemented with 0 and 20 mM Asp (Fig. 4, A and B).

### Nomenclature

AAT genes are named *ASP*, and the isoenzymes are named AAT to distinguish them from the *ASP* genes. There are five *ASP* genes (*ASP1–5*) and three AAT isoenzymes (AAT1–3) in Arabidopsis named according to their mobility through native gels. The major isoenzymes on AAT native gels are AAT2 and AAT3. AAT1, representing the mitochondrial AAT, is a minor component. Mutants in the *ASP* genes that result in defective isoenzyme activity are referred to as *aat* to distinguish them from the wild-type AAT isoenzymes not defective in AAT isoenzyme activity.

### AAT Activity Gel Analysis

Crude protein was extracted from the plants by grinding one leaf in grinding buffer (50 mM Tris, pH 8.0, and  $\beta$ -mercaptoethanol) and sand. After centrifugation, the supernatant was electrophoresed under non-denaturing conditions through a discontinuous PAGE minigel (mini protein II, Bio-Rad, Richmond, CA) for 2 h and stained for AAT activity at room temperature with mild shaking for 15 min. The AAT activity stain was made fresh each time by adding 0.05 g of Fast Blue (F0250, Sigma, St. Louis) to 50 mL of AAT substrate solution (Wendel and Weeden, 1989). AAT substrate solution, pH 7.4, is made of 2.2 mM  $\alpha$ -ketoglutarate (K1875, Sigma), 8.6 mM L-Asp (A6683, Sigma), 0.5% (w/v) polyvinyl pyrrolidone-40 (PVP-40, Sigma), 1.7 mM EDTA (S311-500, Fisher Scientific, Pittsburgh), and 100 mM dibasic sodium phosphate (S-0876, Sigma). Native gels stained for AAT enzyme activity can detect down to 6% of wild-type AAT2 enzyme activity and down to 3% of wild-type AAT3 enzyme activity (Schultz et al., 1998).

### Isolation of T-DNA Mutant

DNA pools of T-DNA representing 60,480 inserted lines from Wisconsin were screened using PCR and primers to the non-coding region of the *ASP2* gene, BM118 AAGAC-GACTTCTCTTTTAACTTATTCCT, and to the T-DNA left border, JL-202 CATTTATAATAACGCTGCGGACATC-TAC. The putative T-DNA mutant was amplified using PCR, cleaned using QIAquick (QIAGEN, Valencia, CA), and sent for sequencing (North Shore University Hospital, Manhasset, NY). The insertion site of the T-DNA was determined to be in the eighth intron of the *ASP2* gene. Hemizygosity (Fig. 1B, lane 2) was determined by PCR using primers BM118 and BM119 CTTAGAAACGGTATGATCTCAATGTCAC located outside the T-DNA insertion site and in the non-coding region of the *ASP2* gene. Amplification of the wild-type gene product was verification of heterozygosity. To test whether there was a single T-DNA insertion in the genome, seed from the *aat2-T* hemizygous mutant (AAT2/*aat2-T*) was sown on Murashige and Skoog plates supplemented with 100 mg mL<sup>-1</sup> kanamycin and the ratio of plants resistant to kanamycin:plants sensitive to kanamycin were scored as 3:1 representing a single T-DNA insertion. Kanamycin is an antibiotic for which the T-DNA has a resistance marker.

### RT-PCR

Total RNA was extracted as previously mentioned and the procedure for RT-PCR was performed as described by the suppliers (Superscript II, 18064-022, Life Technologies/Gibco-BRL, Cleveland).

To determine whether the *ASP2* transcript was properly processed, primers BM74 AGGGAAGCCTCTTGTTCTTG and BM37 TGGCTCTCAACCTTACTAGC to the *ASP2* gene in the coding sequence around the T-DNA insertion site in intron 8 were used to amplify the cDNA product from the RT-PCR reaction. Co-amplification of *ASP5* in the same PCR reaction was used as a positive control. The negative control consisted of all the components of the PCR reaction minus the template. Semiquantitative RT-PCR was accomplished by removing aliquots of the PCR reaction at 25 and 30 cycling times.

### Determination of Missense Mutations in *aat* Mutants

Gene-specific primers were designed to PCR amplify 500-bp regions of the cytosolic *ASP2* and chloroplast *ASP5* genes from the cytosolic *aat2* and chloroplast *aat3* mutants' genomic DNA, respectively, with 50-bp overlapping regions. The amplified regions were cleaned as described (QIAquick, QIAGEN) and sequenced (North Shore University Hospital). Each region was amplified and sequenced four to eight times to ensure the base change was real and not a result of a PCR artifact. Sequences of these *ASP* genes from the *aat* mutants were compared with those from wild type to identify the molecular lesions and their location using GeneWorks software (Oxford Molecular Group, Oxford). DNA sequences were converted to

amino acid sequences and the missense mutations were determined.

### DNA and RNA Analyses

Genomic DNA was extracted as previously described (Ausubel et al., 1987). Shoot tissue and root tissues from the *aat2* and *aat3* mutants were frozen separately in liquid nitrogen and total RNA was extracted using a phenol/chloroform extraction protocol (Jackson and Larkins, 1976). Single-stranded digoxigenin (DIG)-labeled DNA probes were generated according to the manufacturer's specifications (Boehringer Mannheim Biochemicals, Indianapolis). DIG-labeled probes specific to *ASP1-4* were made as previously described (Schultz and Coruzzi, 1995). The *ASP5* DIG-labeled probe was generated using PCR and primers M13R AACAGCTATGACCATG and BM1 TTGCTCCAGG-GAAATAACGC. Northern-blot analyses were performed as described (Sambrook et al., 1989) and hybridization of the DIG-labeled probes was performed at 42°C in ULTRA-hyb solution (8670, Ambion, Austin, TX) for at least 16 h. Post-hybridization washes at 65°C and chemiluminescent detection were conducted according to the manufacturer's specifications (Boehringer Mannheim Genius System User's Guide).

### Amino Acid Analysis of *aat* Mutants Using HPLC

The levels of amino acids in wild-type plants and new additional mutant plants in AAT (*aat2-5*, *aat3-4*, and *aat2-T*) were determined using HPLC. All of the error bars in the HPLC analyses represent SD between three biological replicates. First, the plants were light grown or dark grown for 7 d, unless otherwise noted, harvested, weighed, and frozen in liquid nitrogen. The amino acids were extracted with methanol and chloroform, spiked with nor-Val as a control for the loss of amino acids during extraction, the aqueous phase was vacuum evaporated, and the pellet was resuspended in a volume of water and filtered before HPLC analysis as previously described (Schultz et al., 1998). Samples were derivatized with *O*-phthaldialdehyde at 4°C immediately before injection by an autosampler and separated by reverse-phase HPLC (SCL-10A, Shimadzu, Tokyo) on a C<sub>18</sub> column (Supelcosil LC-18, 25 cm × 4.6 mm, 5 μm, Supelco, Bellefonte, PA) at room temperature. The amino acids were separated using the following gradient of buffer B (72% [v/v] methanol) to buffer A (phosphate buffer, pH 6.86), beginning with 27.5% (v/v) buffer B and finishing with 100% (v/v) buffer B. The gradient used was as follows (time, buffer B [%]): 0.01 min, 27.5% (v/v) B; 38.00 min, 27.5% (v/v) B; 39.00 min, 33% (v/v) B; 63.00 min, 53% (v/v) B; 70.00 min, 59% (v/v) B; 130.00 min, 60% (v/v) B; 135.00 min, 65% (v/v) B; 145.00 min, 100% (v/v) B; 155.00 min, 100% (v/v) B; 160.00 min, 27.5% (v/v) B; 165.00 min, 27.5% (v/v) B; and 165.01 min, stop. The flow rate was 1 mL min<sup>-1</sup>. Derivatized and separated amino acids were detected using an LS30 fluorometer (excitation 340 and emission wavelength 455, Perkin-Elmer Applied Biosystems, Foster City, CA). Amino acid standards (Sigma, LAA-21)

were used to determine the response of each amino acid present at 1,000, 500, 250, 125, and 62.5 pmol. All of the amino acid standards gave a linear correlation of peak area to concentration as determined by linear regression.

Received March 1, 2002; returned for revision March 6, 2002; accepted March 13, 2002.

### LITERATURE CITED

- Ausubel FM, Brent R, Kingston RE, Moore DD, Seiden JG, Smith JA, Struhl K** (1987) Current Protocols in Molecular Biology. John Wiley and Sons, Inc., New York, pp 2.3.1–2.3.7
- Barczak AJ, Jianmin Z, Pruitt KD, Last RL** (1995) 5-Fluoroindole resistance identifies tryptophan synthase beta subunit mutants in *Arabidopsis thaliana*. *Genetics* **140**: 303–313
- Cooper AJL, Meister A** (1985) Metabolic significance of transamination. In P Christen, DE Metzler, eds, *Transaminases*. John Wiley and Sons, Inc., New York, pp 534–561
- Given CV** (1980) Aminotransferases in higher plants. In BJ Mifflin, ed, *The Biochemistry of Plants*, Vol 5. Academic Press, New York, pp 329–357
- Goldberg JM, Swanson RV, Goodman HS, Kirsch JF** (1991) The tyrosine-225 to phenylalanine mutation of *Escherichia coli* aspartate aminotransferase results in an alkaline transition in the spectrophotometric and kinetic  $pK_a$  values and reduced values of both  $k_{cat}$  and  $K_m$ . *Biochemistry* **30**: 305–312
- Hirel B, Lea PJ** (2001) Ammonia assimilation. In PJ Lea, J-F Morot-Gaudry, eds, *Plant Nitrogen*. Springer-Verlag, Berlin, pp 79–99
- Hrazdina G, Jensen RA** (1992) Spatial organization of enzymes in plant metabolic pathways. *Annu Rev Plant Physiol Plant Mol Biol* **43**: 241–267
- Hrmova M, Fincher G** (2001) Plant enzyme structure. Explaining substrate specificity and the evolution of function. *Plant Physiol* **125**: 54–57
- Huang X, Holden HM, Raushel FM** (2001) Channeling of substrates and intermediates in enzyme-catalyzed reactions. *Ann Rev Biochem* **70**: 149–180
- Inoue K, Kuramitsu S, Okamoto A, Hirotsu K, Higuchi T, Kagamiyama H** (1991) Site-directed mutagenesis of *Escherichia coli* aspartate aminotransferase: role of Tyr70 in the catalytic processes. *Biochemistry* **30**: 7796–7801
- Jackson AO, Larkins BA** (1976) Influence of ionic strength, pH, and chelation of divalent metals on isolation of polyribosomes from tobacco leaves. *Plant Physiol* **57**: 5–10
- Kamitori S, Okamoto A, Hirotsu K, Higuchi T, Kuramitsu S, Kagamiyama H, Matsuura Y, Katsube Y** (1990) Three-dimensional structures of aspartate aminotransferase from *Escherichia coli* and its mutant enzyme at 2.5 Å resolution. *J Biochem* **108**: 175–184
- Kirsten H, Gehring H, Christen P** (1983) Crystalline aspartate aminotransferase: lattice-induced functional asymmetry of the two subunits. *Proc Natl Acad Sci USA* **80**: 1807–1810

- Kohler E, Seville M, Jager J, Fotheringham I, Hunter M, Edwards M, Jansonius JN, Kirschner K** (1994) Significant improvement to the catalytic properties of aspartate aminotransferase: role of hydrophobic and charged residues in the substrate binding pocket. *Biochemistry* **33**: 90–97
- Krysan PJ, Young JC, Sussman MR** (1999) T-DNA as an insertional mutagen in *Arabidopsis*. *Plant Cell* **11**: 2283–2290
- Lam H-M, Coschigano K, Schultz C, Melo-Oliveira R, Tjaden G, Oliveira I, Ngai N, Hsieh M-H, Coruzzi G** (1995) Use of *Arabidopsis* mutants and genes to study amide amino acid biosynthesis. *Plant Cell* **7**: 887–898
- Lam H-M, Hsieh M-H, Coruzzi G** (1998) Reciprocal regulation of distinct asparagine synthetase genes by light and metabolites in *Arabidopsis thaliana*. *Plant J* **16**: 345–353
- Lam H-M, Peng SS-Y, Coruzzi GM** (1994) Metabolic regulation of the gene encoding glutamine-dependent asparagine synthetase in *Arabidopsis thaliana*. *Plant Physiol* **106**: 1347–1357
- McPhalen CA, Vincent MG, Picot D, Jansonius JN** (1992) Domain closure in mitochondrial aspartate aminotransferase. *J Mol Biol* **227**: 197–213
- Mehta PK, Hale TI, Christen P** (1989) Evolutionary relationships among homologous proteins. *Eur J Biochem* **186**: 249–253
- Murashige T, Skoog F** (1962) A revised medium for rapid growth and bio assays with tobacco tissue cultures. *Physiol Plant* **15**: 473–497
- Okamoto A, Higuchi T, Hirotsu K, Kuramitsu S, Kagamiyama H** (1994) X-ray crystallographic study of pyridoxal 5'-phosphate-type aspartate aminotransferases from *E. coli* in open and closed form. *J Biochem* **116**: 95–107
- Pan Q-W, Tanase S, Fukumoto Y, Nagashima F, Rhee S, Rogers PH, Arnone A, Morino Y** (1993) Functional roles of valine 37 and glycine 38 in the mobile loop of porcine cytosolic aspartate aminotransferase. *J Bio Chem* **268**: 24758–24765
- Salerno C, Fasella P, Fahien LA** (1985) Transaminases. In P Christen, DE Metzler, eds, *Interaction of Aminotransferases with Other Metabolically Linked Enzymes*. John Wiley and Sons, Inc., New York, pp 196–197
- Sambrook J, Fritsch EF, Maniatis T** (1989) *Molecular Cloning: A Laboratory Manual*. Cold Spring Harbor Laboratory Press, Plainview, NY
- Schultz CJ, Coruzzi GM** (1995) The aspartate aminotransferase gene Family of *Arabidopsis* encodes isoenzymes localized to three distinct subcellular compartments. *Plant J* **7**: 61–75
- Schultz CJ, Meier H, Miesak B, Coruzzi GM** (1998) *Arabidopsis* mutants define an *in vivo* role for isoenzymes of aspartate aminotransferase in plant nitrogen assimilation. *Genetics* **149**: 491–499
- Smith DL, Almo SC, Toney MD, Ringe D** (1989) 2.8-Å Resolution crystal structure of an active-site mutant of aspartate aminotransferase from *Escherichia coli*. *Biochemistry* **28**: 8161–8167
- Stitt M** (1999) Nitrate regulation of metabolism and growth. *Curr Opin Plant Biol* **2**: 178–186
- Udvardi AA, Kahn ML** (1991) Isolation and analysis of a cDNA clone that encodes an alfalfa (*Medicago sativa*) aspartate aminotransferase. *Mol Gen Genet* **231**: 97–105
- Urquhart AA, Joy KW** (1981) Use of phloem exudate technique in the study of amino acid transport in pea plants. *Plant Physiol* **68**: 750–754
- Wendel JF, Weeden NF** (1989) Isozymes in plant biology. In DE Soltis, PE Soltis, eds, *Visualization and Interpretation of Plant Isozymes*. Discords Press, OR, pp 5–45
- Wilkie SE, Lambert R, Warren MJ** (1996) Chloroplastic aspartate aminotransferase from *Arabidopsis thaliana*: an examination of the relationship between the structure of the gene and the spatial structure of the protein. *Biochem J* **319**: 969–976
- Wilkie SE, Roper JM, Smith AG, Warren MJ** (1995) Isolation, characterization, and expression of a cDNA clone encoding aspartate aminotransferase from *Arabidopsis thaliana*. *Plant Mol Biol* **27**: 1227–1233
- Ziak M, Jager J, Malashkevich VN, Gehring H, Jaussi R, Jansonius JN, Christen P** (1993) Mutant aspartate aminotransferase (K258H) without pyridoxal-5'-phosphate-binding lysine residue structural and catalytic properties. *Eur J Biochem* **211**: 475–484